Electronic and optical properties of nitrogen-doped multiwalled carbon nanotubes

S. H. Lim,[1,2] H. I. Elim,[3] X. Y. Gao,[2] A. T. S. Wee,[2] W. Ji,[2] J. Y. Lee,[3] and J. Lin[1,2,*]
[1]*Applied Catalysis, Institute of Chemical and Engineering Sciences, Singapore 627833*
[2]*Department of Physics, National University of Singapore, Singapore 119260*
[3]*Department of Chemical and Biomolecular Engineering, National University of Singapore, Singapore 117576*
(Received 19 June 2005; revised manuscript received 21 September 2005; published 4 January 2006)

Highly nitrogen-doped carbon nanotube (CN_xNT, $x=12$ at. %) was synthesized by the pyrolysis of acetonitrile on Co-Mo catalysts. The electronic structures and chemical bondings of CN_xNT were studied using various spectroscopic techniques: Raman, photoelectron and x-ray absorption spectroscopies. The ultrafast pump-probe measurements of CN_xNT exhibited a larger third-order susceptibility $\chi^{(3)}$, a relaxation time of $\tau_2=1$ ps and improved saturable absorption, as compared with undoped multiple-walled carbon nanotubes, which indicate that N-doping can improve all-optical switching properties of carbon nanotubes.

DOI: 10.1103/PhysRevB.73.045402 PACS number(s): 73.22.−f, 78.67.Ch, 79.60.Jv, 61.72.Ff

I. INTRODUCTION

Single-walled carbon nanotubes (SWNTs) are seamlessly rolled-up graphene sheets of carbon and they exhibit a variety of electronic properties, which are greatly dependent on their tubular diameter and chirality. Theoretical and experimental studies show that SWNTs can behave from being metallic to semiconducting ones,[1–3] while those of multiwalled carbon nanotubes (MWNTs) depends on the features of each coaxial carbon shell.[4] Thus these advanced materials are very promising for applications such as nanoelectronics, biosensors, gas storage, and optical communications.[5,6]

The deliberate introduction of defects and impurities (dopants) into carbon nanotube could offer a possible route to change and tune its electronic properties. The creation of new energy levels in the band gap with associated electronic states is an important step to make electronic devices. For instance, the intercalation of alkali metals into SWNT bundles has been shown to increase the conductivity.[7] The substitution of carbon atoms by boron or (and) nitrogen dopants has modified the electrical and structural properties of carbon nanotubes, giving them characteristic bamboo-shaped structures.[8–15]

The synthesis of carbon nitride (CN) nanotubes is of particular interest because they are expected to be metallic, independent of the tubule diameter and chirality. This is motivated by theoretical prediction of the existence of stable CN tubular structures.[16] Thus various approaches have been made to incorporate nitrogen atoms into carbon nanotubes, including magnetron sputtering,[9] pyrolysis of nitrogen-rich organic chemicals,[10–12] and arc discharge in nitrogen atmosphere.[13] But the synthesized nanotubes are still far from the canonical carbon nitride stoichiometric CN. The solubility of nitrogen in graphite layers is reported to be <5 at. % in most of the bulk nitrogen-doped carbon nanotubes (CN_xNT).[13] However high N-content (10–19 at. %) CN_x nanotubes were also identified[11,17] and some nanodomains may contain nitrogen concentration up to 30 at. %.[9] Even these CN_x nanotubes at low doping level already exhibit different electronic and structural properties.

Here we report the spectroscopic studies and ultrafast pump-probe measurements of highly nitrogen-doped ($\sim$12 at. %) carbon nanotubes. The CN_x nanotubes were synthesized by the pyrolysis of acetonitrile on Co-Mo catalysts. TEM, Raman, XPS, UPS, and x-ray absorption techniques (using synchrotron radiation source) were used to characterize and study the chemical bonding and electronic structures of the CN_x nanotubes. Previously, Elim *et al.*[18] reported the degenerate pump-probe measurements of a MWNT film deposited on a quartz substrate and showed that MWNTs were potential ultrafast optical switching materials. However, there is no report on the optoelectronic properties of N-doped MWNTs. Thus we examined the effects of nitrogen dopants on the carbon nanotube's optoelectronic properties using ultrafast pump-probe experiments. A better switching property was measured on our CN_xNT samples, which suggests that these CN_x nanotubes can be used in saturable optical absorber devices. Saturable absorber devices can offer a potential solution for passive optical regeneration, error-free periodically amplified optical transmission and laser mode locking.

II. EXPERIMENTAL

The CN_x nanotube was synthesized by chemical vapor deposition (CVD) technique using Co-Mo catalysts. Acetonitrile (CH_3CN) vapor, which was chosen as the sources of carbon and nitrogen for the CN_x nanotube growth, was carried by a helium (99.9995% purity) flow of 60 sccm. The $Co_{0.05}Mo_{0.025}$ catalyst supported on MgO was prepared via a wet combustion of the correspondent nitrate salts[19] at 700 °C for 30 min. The as-synthesized samples were refluxed in 10 M HCl to remove the metal catalysts.

The purified CN_x nanotubes (CN_x) were characterized with transmission electron microscope (TEM, JEOL JEM-2010J) and Raman spectroscopy (Reinshaw micro-Raman 2000 system, with an excitation laser of 514 nm). XPS, UPS, and XANES measurements were performed at SINS beamline at the Singapore Synchrotron Light Source (SSLS)[20], using photon energy of 700 eV for core levels, 40.8 eV for valence band, and 60 eV for work function studies, respectively. The samples were biased by −10 V during the work function measurements to accelerate the low energy second-

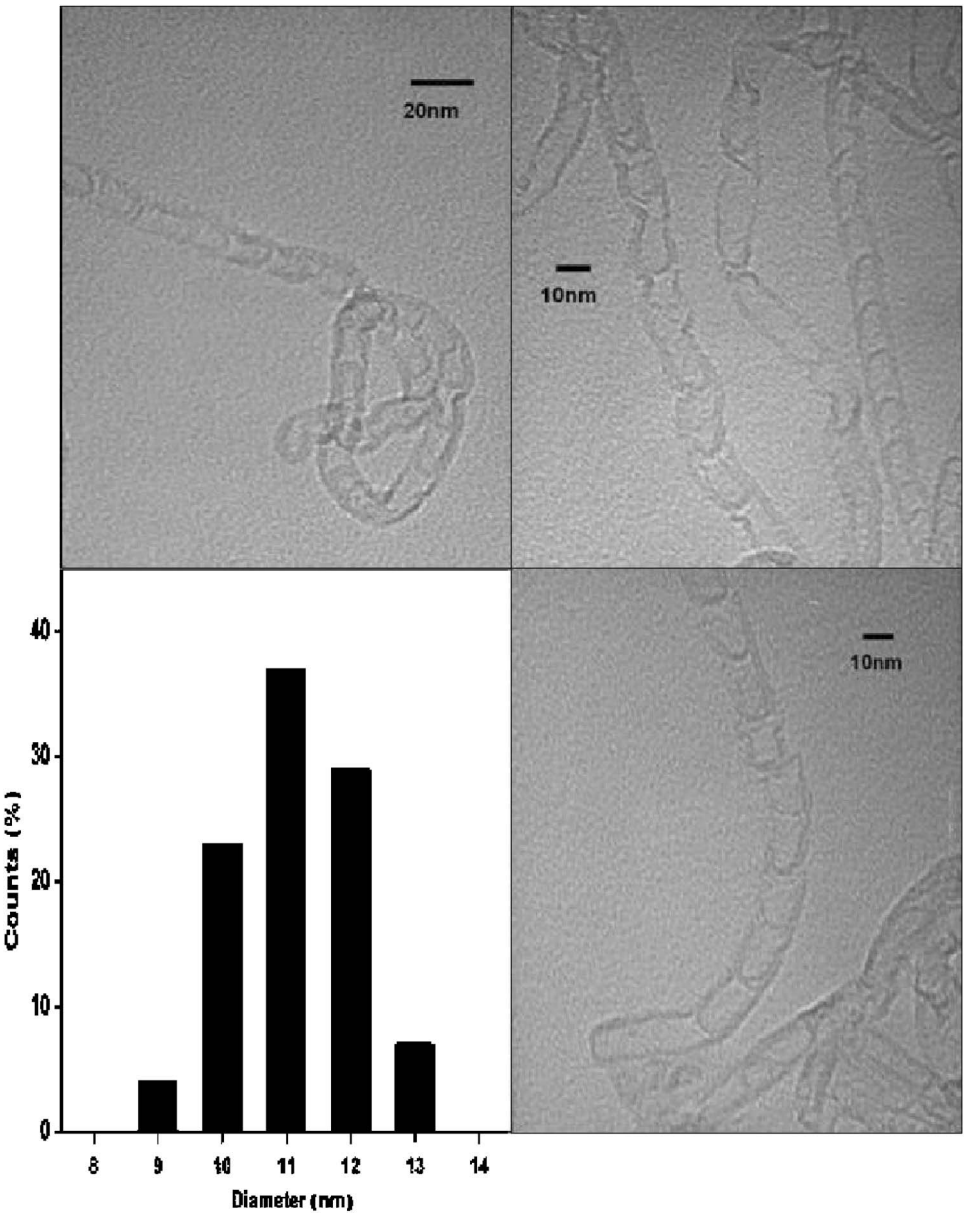

FIG. 1. Typical TEM images of bamboo-shaped nitrogen-doped carbon nanotubes.

ary electrons and to get rid of the influence of analyzer work function. The XANES was measured using a sample drain current in total electron yield mode. For the ultrafast laser pump-probe experiments, a drop of the uniformly dispersed solution of the purified CN_x nanotubes in isopropanol was cast onto a quartz slide to form the CN_x nanotube film. For comparison a thin film of pristine multiwalled carbon nanotubes (MWNTs, purchased from Shenzhen Nanoport with average diameter of $\sim$10 nm) was prepared following the above procedures. As described elsewhere,[18] 100-fs-laser pulses at 1 kHz were employed for the pump-probe studies.

III. RESULTS AND DISCUSSION

The CN_x nanotubes possess a characteristic bamboo-shaped morphology (see Fig. 1). They can be considered as polymerized carbon nitride nanobells, whereby each nanocompartment is linked together to form the tube. Our CN_x samples have a narrow diameter distribution between 9 and 13 nm, with few bamboo-shaped CN_x nanotubes having diameters smaller than 8 nm. The same $Co_{0.05}Mo_{0.025}$ catalysts were used for the synthesis of SWNTs in our lab.[19] However when they were employed for the synthesis of N-doped nanotubes, only CN_x multiwalled nanotubes were obtained, with no bundle of SWNTs. Zhong *et al.*[21] also attempted to synthesize N-doped SWNTs using the laser ablation technique but the SWNTs are not nitrogenated. Nitrogen doping can only be found on the amorphous carbon materials. Based on the theoretical calculation of vacancy-mediated N substitution, Srivastava *et al.*[22] show that pyridinelike vacancy defects and N substitution are favored on the surface of nanotubes with diameters larger than 8 nm. For carbon nanotubes with diameters $<$8 nm, N chemisorption or fused pentagon-type defects occurs. Thus it can be surmised that most of our CN_x nanotubes contains pyridinelike vacancy defects due to N doping.

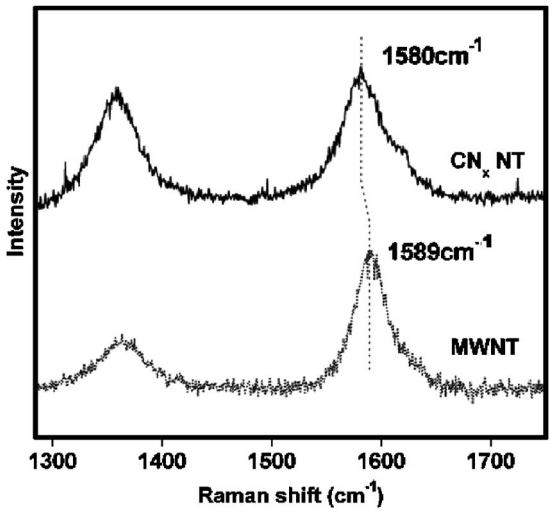

FIG. 2. First-order Raman spectra of the as-synthesized CN_x nanotubes and MWNT.

The Raman spectra of our CN_x nanotubes and MWNTs are plotted in Fig. 2 for comparison. Both consist of the D-band ($\sim$1300 cm^{-1}) and the G-band ($\sim$1600 cm^{-1}) peaks. The I_D/I_G ratio of the MWNTs and CN_x nanotubes are 0.36 and 0.95, respectively. This significant increase in the I_D/I_G ratio strongly implies the presence of nitrogen dopants and defects in CN_x nanotubes. The G band of the CN_x nanotubes shows a down-shift from 1589 to 1580 cm^{-1} in comparison to MWNT, indicating a charge-transfer from the nitrogen dopants to the carbon atoms.[23]

The pristine MWNT sample is free from atmospheric contaminants, showing no signals of XPS O1s and N1s core energy levels. The C1s spectra for the MWNT and CN_x nanotubes are normalized and displayed in Fig. 3(a). A chemical up-shift of 0.2 eV and an asymmetric broadening in the high binding energy tail are observable for the CN_x nanotubes (solid line). The up-shift of the C1s line may result from the presence of N atoms which induce a charge transfer from the less electronegative C to more electronegative N. As such, some homopolar C-C bonds are replaced by heteropolar C-N bonds and caused a shift in the C1s core levels towards higher binding energy.[24] The asymmetric broadening of the C1s peak of the CN_x nanotubes suggests the existence of various carbon species in the higher binding energy regions. By peak analysis two additional peaks can be fitted at 285.6 and 287.1 eV, in addition to the major peak at 284.5 eV [graphitelike C-C bond, see Fig. 3(b)]. It is noted that the N1s peak can also be fitted with two Gaussian lines located at 398.2 and 400.7 eV [see Fig. 3(c)]. According to the suggestion of Marton *et al.*,[25] there are two carbon-nitride phases. In phase 1, which corresponds to the C1s level at 287.1 eV and N1s at 398.2 eV, N atoms are in a sp^3 bonding configuration with an isolated electron lone pairs (similar to β-Si_3N_4). Phase 2 corresponds to the C1s line at 285.6 eV and N1s at 400.7 eV, which represents substitutional N atoms in a sp^2 graphitelike configuration. From the peak intensity analysis a high nitrogen content of $\sim$12 at. % can be estimated. Noted that Glerup *et al.*[11] had attained 16–19.6 at. % N-doped carbon nanotubes using acetonitrile-tetrahydrofuran mixture as the precursor while Nath *et al.*[17] had prepared $C_{10}N$ nanotubes from the pyrolysis of pyridine over Fe/SiO_2.

Because of the one extra 2p electron of each substitutional N atom (as compared to the carbon atoms) N-doped carbon nanotubes are expected to show stronger π bonds of aromatic rings.[24,25] This can be observable in our UPS valence-band (VB) studies. In Fig. 4(a) the VB spectrum of the MWNT sample exhibits two bands located at binding energies 3.1 and 7.6 eV, which correspond to the C2p π and σ electrons respectively as reported in the literature.[26] Upon doping with $\sim$12 at. % nitrogen, both π and σ bands shift

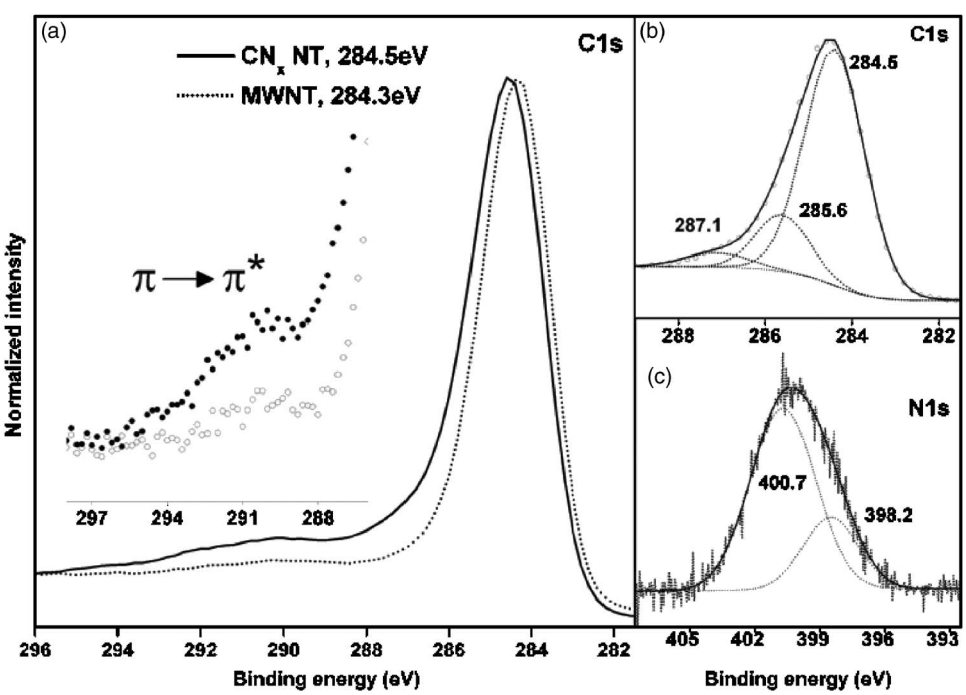

FIG. 3. (a) XPS C1s core level spectra for pristine MWNT (dotted line) and N-doped carbon nanotube (solid line) with 12 at % N-dopant. Inset: Energy loss due to the $\pi \rightarrow \pi^*$ transition. (b) and (c) Deconvolved C1s and N1s spectra for CN_x nanotubes, $x \approx 12$ at %.

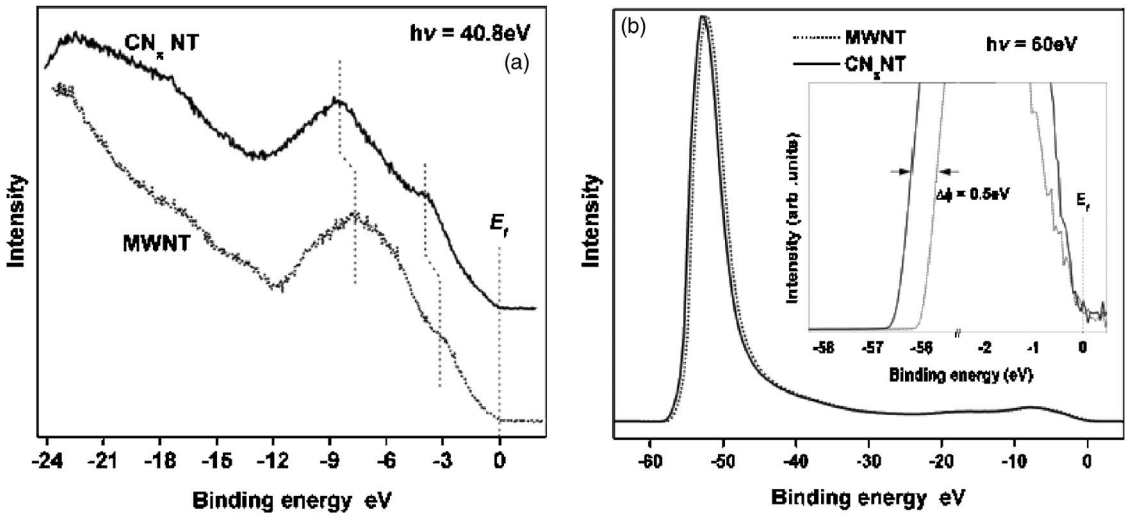

FIG. 4. (a) UPS He II (40.8 eV) valence band spectra of pristine MWNT and N-doped CNT. (b) Secondary electron tail threshold spectra of pristine MWNT and N-doped CNT using photon energy=60 eV. Inset: Expanded view of the secondary electron tail threshold and top valence band regions.

rigidly towards higher binding energies by ~0.5 eV. This shift can be attributed to the rise of Fermi level due to N doping. Each nitrogen atom has five valence electrons vs four per carbon. The substitution of electron-rich nitrogen into the carbon network therefore would include a donor level near the bottom of the conduction band, raising the Fermi level.[27] After correction of the Fermi level shift, the intensity enhancement of the π-derived peak at ~3 eV is obvious in the CN_x spectrum. The enhancement of the π peak is related to the fact that each sp^2 N atom can contribute two electrons to the π system as compared to one π electron per network carbon atom. The σ-like peak at 7 eV decreases its intensity whereas an increase in the intensity around 17 eV is evident too. This may also reflect the substitution of C-C bonds by C-N bonds.[28,29] More XPS evidence of the N substitution is the observation of an extra energy loss peak in the C1*s* region, which is located ~6 eV at the higher binding energy and corresponds to $\pi \rightarrow \pi^*$ electron transition [see Fig. 3(a) inset]. A similar observation was reported for amorphous a-CN_x:H film as its nitrogen content was increased.[24]

The secondary electron tail threshold regions of pristine MWNTs and CN_x nanotubes were presented in Fig. 4(b). The secondary electron tail threshold of the CN_x nanotubes is shifted 0.5 eV towards higher binding energy in comparison to that of MWNT, which means a reduction of work function by 0.5 eV. This is consistent to the rise of Fermi level [in Fig. 4(a)] due to the N doping. Additionally as shown in the inset of Fig. 4(b), the nitrogen substitution has enhanced the leading edge of the valence band in a large binding energy region (up to 3 eV), which may be associated to the N lone pair.[28] Both the reduction in work function and the enhancement of the electron density at the top valence band bear great importance to improve the field-emission properties of CNTs.[10] Our results are in good agreement with first-principles calculations, which predict a 0.18 eV reduction in the work function of CNT when a nitrogen atom is substituted in the tip.[29] The greater reduction in work function as determined by us could be due to the unique polymerized nanobell structures of CN_x nanotubes whereby the linking compartmentalized regions are usually enriched with nitrogen and reduced the work function more as compared to tip substitution.

X-ray absorption near-edge spectroscopy (XANES) is employed to further probe the electronic structure of the CN_x nanotubes. Figure 5 shows the carbon *K* edge of the MWNTs and CN_x nanotubes. Both spectra exhibit two peaks at ~285 and ~292 eV, which are related to the graphitic C1*s*-C $2p\pi^*$ and C1*s*-C$2p\sigma^*$ resonance, respectively. A detailed observation shows that the C1$s \rightarrow \pi^*$ peak of the CN_x nanotubes (solid line in Fig. 5 inset) is up shifted by 0.3 eV. By considering the 0.5 eV rising of the Fermi level in the CN_x nanotubes, both C1*s* and C $2p\pi^*$ in the CN_x nanotubes are actually shifted up by 0.3 eV as compared to those of pristine MWNTs. This can be attributed to the upward band

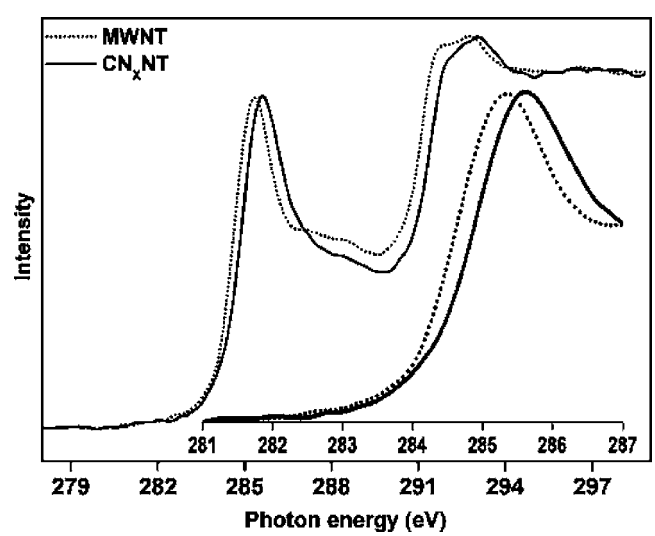

FIG. 5. XANES C1*s* *K*-edge absorption spectra of pristine MWNTs (dotted lines) and CN_x nanotubes (solid lines). Inset: An expanded view of the graphitic C1$s \rightarrow \pi^*$ resonance.

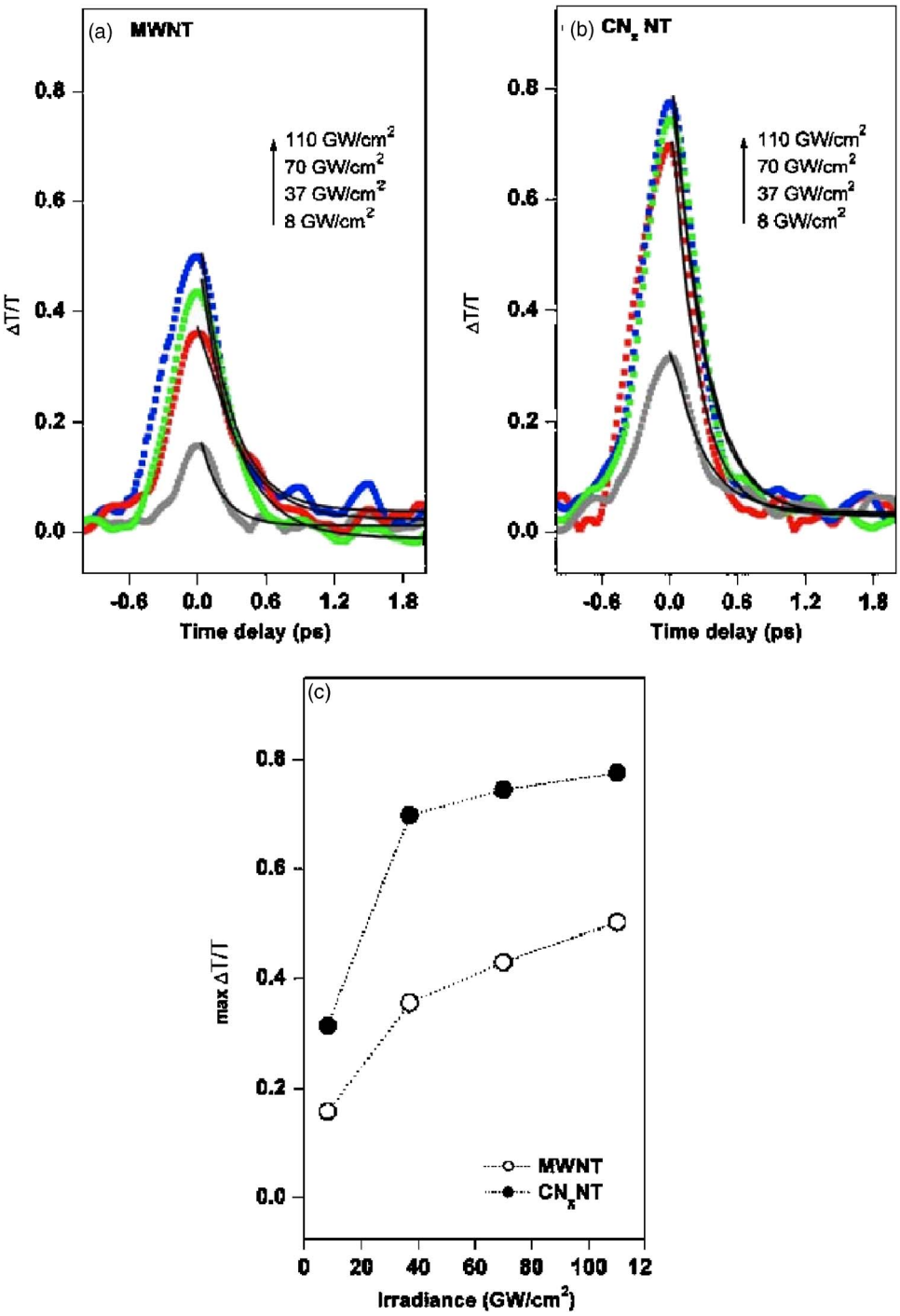

FIG. 6. (Color online) Degenerate 130-fs time-resolved pump-probe measurements of (a) pristine MWNT and (b) CN_x nanotubes performed at 780 nm with increasing irradiance. All the solid lines in (a) and (b) are two-exponential fitting curves with $\tau_1 = 130$ fs and $\tau_2 = 1$ ps. (c) A plot of maximum $\Delta T/T$ against irradiance for MWNT and CN_xNT.

bending. Substituting N atoms behave as dopants of the n-type semiconductor on one hand, but, since N is more electronegative than carbon atoms, they can provide accepterlike state on the other hand. This would result in upward band bending.

Figures 6(a) and 6(b) shows the typical one color pump-probe data of the MWNT and CN_x nanotubes samples taken at the same wavelength of 780 nm with increasing irradiance of 8, 37, 70, and 110 GW/cm^2. All the signals show a positive change in transmission which is related to photoinduced bleaching. Furthermore, the transient signals clearly show there are two components. By using a two-exponential component model, the best fits [solid lines in Figs. 6(a) and 6(b)] produce $\tau_1 = 130$ fs and $\tau_2 = 1$ ps. We believe that τ_1 is the autocorrelation of the laser pulses used. The τ_2 component is the recovery time of the excited π electrons in the CN_x nanotubes film. It should be pointed out that the relaxation dynamics are not dependent on the pump irradiance, including the saturation regime. Its time scale is comparable to the findings for SWCNTs.[20]

However, as shown in Fig. 6(c), we have observed that the pump irradiance dependence of the maximum value of $\Delta T/T$ in the CN_x nanotubes is greater than that in MWNT. This confirms the results that the larger third-order suscepti-

bility of CN_x nanotubes is due to the presence of nitrogen dopants. The observed larger third-order susceptibility is attributed to higher-density π electrons of CN_x nanotubes as elucidated by XPS energy loss and valence band spectra [Figs. 3(a) and 4(a)].

It is observed that the positive $\Delta T/T$ signals develop as the irradiances increase. However when the irradiances increase from 37 to 110 GW/cm^2, the maximum $\Delta T/T$ signals of CN_xNT remain almost the same. Figures 6(a)–6(c) give a clear sign of saturation in CN_xNT. In this saturation regime, most of the carrier states of CN_x nanotubes are filled and thus the sample absorption is completely quenched. A similar observation has been made on semiconducting SWNT in a very low fluence of 1 mJ/cm^2 ($\sim$7 GW/cm^2). On the other hands, pristine MWNT did not show clear absorption saturation.

The better ultrafast saturable absorption of CN_x nanotubes suggests that these CN_x nanotubes can be used as saturable absorber devices. With improved fabrication techniques, saturable absorber devices based on CN_x nanotubes can offer a potential solution for passive optical regeneration, error-free transmission distances of periodically amplified optical transmission systems, laser mode locking based on saturable absorber, and high noise suppression capability. For examples, Set and Yamashita *et al.*[30,31] have already explored the application of saturable absorbers involving SWNTs.

IV. CONCLUSION

Highly nitrogen-doped carbon nanotubes ($\sim$12 at. %) were synthesized by pyrolysis of acetonitrile on Co-Mo catalysts. Photoemission studies show that the whole valence band is shifted to deeper binding energy due to the nitrogen doping which causes Fermi level shifts to conduction band edge. The work function of carbon nanotubes is reduced by 0.5 eV. The enhancement of electron density near the top of valence band, the rise of the valence band π peak and the decay of the valence band σ peak are all related to the N substitution to the carbon network. Consequently the richer density of π electrons in CN_x NTs endows it with larger third-order susceptibility and better ultrafast saturable absorption.

*Email address: lin_jianyi@ices.a-star.edu.sg

[1] J. W. Mintmire, B. I. Dunlap, and C. T. White, Phys. Rev. Lett. **68**, 631 (1992).
[2] N. Hamada, S. I. Sawada, A. Oshiyama, Phys. Rev. Lett. **68**, 1579 (1992).
[3] T. W. Odom, J. Huang, P. Kim, and C. M. Lieber, Science **391**, 62 (1998).
[4] M. Ge and K. Sattler, Science **260**, 515 (1993).
[5] R. Andrews, D. Jacques, D. Qian, and T. Rantell, Acc. Chem. Res. **35**, 1008 (2002).
[6] M. Ouyang, J.-L. Huang, and C. M. Lieder, Acc. Chem. Res. **35**, 1018 (2002).
[7] R. S. Lee, H. J. Kim, J. E. Fischer, A. Thess, and R. E. Smalley, Nature (London) **388**, 255 (1997).
[8] R. Sen, B. C. Satishkumar, A. Govindaraj, K. R. Harikumar, G. Raina, J. Zhang, A. K. Cheetham, and C. N. R. Rao, Chem. Phys. Lett. **287**, 671 (1998).
[9] K. Suenage, M. P. Johansson, N. Hellgren, E. Broitman, L. R. Wallenberg, C. Colliex, J. Sundgren, and L. Hultman, Chem. Phys. Lett. **300**, 695 (1999).
[10] C. Tang, D. Golberg, Y. Bando, F. Xu, and B. Liu, Chem. Commun. (Cambridge) **24**, 3050 (2003).
[11] M. Glerup, M. Castignolles, M. Holzinger, G. Hug, A. Loiseau, and P. Bernier, Chem. Commun. (Cambridge) **20**, 2542 (2003).
[12] S. Trasobares, O. Stephan, C. Colliex, W. K. Hsu, and H. W. Kroto, J. Chem. Phys. **116**, 8966 (2002).
[13] R. Droppa, Jr., C. T. M. Ribeiro, A. R. Zanatta, M. C. dos Santos, and F. Alvarez, Phys. Rev. B **69**, 045405 (2004).
[14] G. G. Fuentes, E. Borowiak-Palen, M. Knupfer, T. Pichler, J. Fink, L. Wirtz, and A. Rubio, Phys. Rev. B **69**, 245403 (2004).
[15] D. Golberg, Y. Bando, L. Bourgeois, K. Kurashima, and T. Sato, Carbon **38**, 2017 (2000).
[16] Y. Miyamoto, M. L. Cohen, and S. G. Louie, Solid State Commun. **102**, 605 (1997).
[17] M. Nath, B. C. Satishkumar, A. Govindaraj, C. P. Vinod, and C. N. R. Rao, Chem. Phys. Lett. **322**, 333 (2000).
[18] H. I. Elim, W. Ji, G. H. Ma, K. Y. Lim, C. H. Sow, and C. H. A. Huan, Appl. Phys. Lett. **85**, 1799 (2004).
[19] S. Tang, Z. Zhong, Z. Xiong, L. Sun, L. Liu, Z. X. Shen, and K. L. Tan, Chem. Phys. Lett. **350**, 19 (2001).
[20] X. J. Yu, O. Wilhelmi, H. O. Moser, S. V. Vidyarai, X. Y. Gao, A. T. S. Wee, T. Nyunt, and H. Zheng, J. Electron Spectrosc. Relat. Phenom. **144**, 1031 (2005).
[21] Y. Zhang, H. Gu, and S. Iijima, Appl. Phys. Lett. **73**, 3827 (1998).
[22] D. Srivastava, M. Menon, C. Daraio, S. Jin, B. Sadanadan, and A. M. Rao, Phys. Rev. B **69**, 153414 (2004).
[23] P. W. Chiu, G. S. Duesberg, U. Dettlaff-Weglikowska, and S. Roth, Appl. Phys. Lett. **80**, 3811 (2002).
[24] A. Mansour and D. Ugolini, Phys. Rev. B **47**, 10 201 (1993).
[25] D. Marton, K. J. Boyd, A. H. Al-Bayati, S. S. Todorov, and J. W. Rabalais, Phys. Rev. Lett. **73**, 118 (1994).
[26] J. Ago, T. Kugler, F. Cacialli, W. R. Salaneck, M. S. P. Shaffer, A. H. Windle, and R. H. Friend, J. Phys. Chem. B **103**, 8116 (1999).
[27] R. Czerw, M. Terrones, J.-C. Charlier, X. Blase, B. Foley, R. Kamalakaran, N. Grobert, H. Terrones, D. Tekleab, P. M. Ajayan, W. Blau, M. Ruhle, and D. L. Carroll, Nano Lett. **9**, 457 (2001).
[28] S. Souto, M. Pickholz, M. C. dos Santos, and F. Alvarez, Phys. Rev. B **57**, 2536 (1998).
[29] G. Zhang, W. Duan, and B. Gu, Appl. Phys. Lett. **80**, 2589 (2002).
[30] S. Y. Set, H. Yaguchi, Y. Tanaka, and M. Jablonski, J. Lightwave Technol. **22**, 51 (2004).
[31] S. Yamashita, Y. Inoue, S. Maruyama, Y. Murakami, H. Yaguchi, M. Jablonski, and S. Y. Set, Opt. Lett. **29**, 1581 (2004).